3D printed smart repairs for civil infrastructure

Christos Vlachakis, Lorena Biondi, Marcus Perry
Department of Civil and Environmental Engineering, University of Strathclyde,
Glasgow, G1 1XJ, United Kingdom
christos.vlachakis@strath.ac.uk

Abstract

This paper outlines the development of 3D printed smart materials for civil infrastructure repair and monitoring. The materials employed in this project are metakaolin-based geopolymers, characterized as "smart" due to their ability to simultaneously sense and repair steel and concrete structures. As metakaolin geopolymers attain comparable mechanical properties to ordinary Portland cement and favourable adhesive characteristics, they can be used to restore the structural integrity of degraded concrete elements. Geopolymers furthermore exhibit a pronounced electrical conductivity due to the presence of free ions in their matrix. Geopolymers can therefore be used to detect variations in strain and temperature through changes in electrical impedance. In essence, these are repair materials that also enable constant monitoring. In this project, smart materials are being extruded with the assistance of a 3D printer, and will ultimately be robotically applied. The extrusion of smart cement patches via a 3D printer allows greater versatility of design and improved geometrical repeatability. Patch shape and size can be easily adjusted according to the requirements of each given circumstance, while robotics will allow printing in areas with hazards or limited access. In this paper, we will present our latest progress in printing and characterising the mechanical and electronic properties of geopolymer patches, and discuss how raw sensor data can be interpreted into measures of structural health. We will also outline the challenges in the system's design, and describe the future work required to scale the technology up to real industrial applications.

1. Introduction and technical background

Geopolymers have been considered a viable alternative to ordinary Portland cement (OPC) and epoxy concrete repairs due to their low embodied carbon and their comparable mechanical and technical properties [1–3]. The term geopolymer was first introduced by Davidovits in 1978 following his research in fire resistant materials[4]. In recent years, geopolymers have been considered to be part of a larger category of materials called 'alkali activated materials'[5]. Alkali activated materials are formed through the reaction of an aluminosilicate precursor usually metakaolin or fly ash and an alkali solution [6,7].

Metakaolin is produced through the calcination of pure kaolin between 500 ^{o}C and 900 ^{o}C between 1-24h depending on the exact calcination temperature[6]. This process can be carried out either by using a rotary kiln or by flash calcination[8]. As metakaolin is a raw material and not an industrial by-product, it exhibits a more consistent behaviour than fly ash. That said, one of the major issues associated with metakaolin-based geopolymer is its poor workability which has limited its application to adhesives and coatings over the years[6,9]. While the addition of water enhances workability at the same time this also

lowers the material's strength[9]. In general, mixes with more solid than liquid content are practically unworkable[10]. The properties of geopolymers are controlled by the viscosity of the alkali solution. Potassium based solutions have been stated to produce more workable mixes[3]. Employing plasticizers up to 3% can increase workability without any drawbacks to mechanical properties[11]. On the other hand traditional admixtures [12] and additives such as sodium polacrylate [13] have not been known to reduce viscosity.

Apart from a structural stand point of view, geopolymers have also been used as a sensing material in structural health monitoring applications. Geopolymers have been used as a smart adhesive to act as a deformation sensing element [14], a self-sensing element [15], and in hybrid applications to detect strain and temperature variations through changes in electrical impedance[16]. This is feasible on account of the electrical conductivity the material exhibits due to the residual alkali activator in its pores. The conductivity of geopolymers is that of a semi-conductor material[17]. Liquid ratio[18], the water molecules and hydroxide at room temperature[17] are factors that affect conductivity in geopolymers. Lastly, materials such as carbon fibers[19] and graphene oxide[15] have been used to increase the conductivity of geopolymers.

A recent approach to geopolymer casting and cementitious materials alike is additive manufacturing. This method allows great design versatility and geometrical repeatability. The shape and size of each extruded object can be easily adjusted to meet the requirements of the given circumstance. Technologies such as stereolithography, fused deposition modelling and contour crafting have been applied to create printed concrete samples[20]. In order to successfully carry out concrete additive manufacturing the mix used must attain the following four attributes: pumpability, printability, buildability and open time[21,22]. A brief description of each characteristic is presented further below.

1. Pumpability or workability refers to the flow of the material and the ability be transferred.
2. Printability or extrudability is the ability a material has to be extruded as a continuous filament.
3. Buildability refers to the number of layers that can be extruded without leading to any deformation. In essence it is the resistance to deform under load.
4. Open time is related to the setting time of cementitious materials. It is the period of time where the material's properties remain the same.

In this research the electric response of a 3D printed metakaolin-based geopolymer is investigated.

2. Methodology

This section outlines the procedure for producing, extruding, casting and electronically testing metakaolin geopolymer samples.

2.1 Metakaolin production

For this study metakaolin was produced by calcining highly refined china clay in an electric furnace at 800 ^{o}C for 2 hours[23]. The properties of the clay are presented in table 1.

The precursor was left to cool in the furnace and then removed and stored in sealed containers prior to use. The mass ratio of the alkali activator used for this experiment was Na_2SiO_3: NaOH =2.0. The solution was left to rest for at least 24h before being used.

Table 1 Kaolin properties

Origin	SiO_2	Al_2O_3	Mean particle size
Southwest England,UK	47% mass	38% mass	10 μm

Metakaolin geopolymer was made by pouring the activator solution into the metakaolin precursor and mechanically mixing for at least 10 minutes until a homogeneous mix was obtained. The batch was occasionally manually mixed until used for extrusion.

2.2 Printing setup

To allow geopolymer extrusion and 3D printing, a progressive cavity dosing pen was installed onto the x-y stage of a 3D printer. The material for extrusion was inserted into the cartridge as depicted in figure 1.

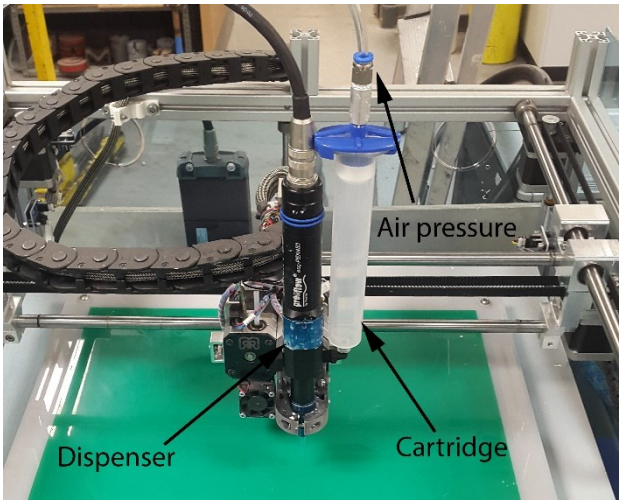

Figure 1. 3D printing setup

2.3 Mix design

In order to determine the optimal solid-to-liquid ratio that would be used two mixes were prepared and were examined for the characteristics of additive manufacturing. The mixes that were prepared had a solid-to-liquid ratio of 0.8 (wet batch) and 0.9 (dry batch), table 2. In addition to the additive manufacturing attributes, three separate nozzle sizes 14G (1.60mm), 16G (1.22mm) and 18G (0.84mm) were also examined for each batch. The characteristics examined as previously mentioned were extrudability, buildability, open time and workability.

Upon completing this procedure, an optimal mix would be determined to continue with EIS testing.

Table 2. Batch content

Batch name	Solid-to-liquid content ratio
Wet batch	0.8
Dry batch	0.9

2.4 Extrusion

A rectangular prism with dimensions 25 mm x 60 mm x 4 mm was to be printed for each combination of parameters above. A total of six prisms were printed.

An stl file in CAD software of the patch was prepared and inserted into a slicing software to generate the G-code for extrusion. A printing speed of 25 mm/s was selected along with 50% rectilinear infill density. The objects were printed directly onto the printer's surface bed. Once the optimal mix was determined the patch was printed onto a non-conductive plastic ruler with four glued electrodes onto it at 10 mm spacing each for impedance testing.

2.5 Curing

The printed sample were sealed and cured in an environmental chamber at 20 ^{o}C and 80% relative humidity until testing. Upon testing, the sample was placed back into a container and kept at room temperature.

2.6 Electrical testing

The electronic impedance of the sample was tested with an electrical impedance analyser using a four-probe set up. The samples were placed in a Faraday cage to eliminate any potential interferences and tested under potentiostatic electrochemical impedance spectroscopy between 0.1 Hz and 1 MHz.

3. Results and Discussion

In this section, the results of the mix selection are presented along with the EIS responses of a casted and printed metakaolin geopolymer sample.

3.1 3D printing mix

3.1.1 Solid-to-liquid ratio

In regards to the wet batch, as illustrated in figure 2a, it can be easily distinguished that this ratio cannot produce great detail nor can it satisfactorily achieve the desired shaped. Its curvy edges are a result of poor buildability unable to retain its shape upon every new layer. On the other hand, this batch exhibited great printability as no extrusion issues were observed in any object. Furthermore, this mix design also had fairly good workability during mixing and during insertion into the syringe barrel. Lastly, open time did not seem

to be an issue as the material did not significantly change between mixing and loading into the cartridge.

This is distinct from the results for the dry batch, shown in figure 2b. This mix produced high-quality prints achieving the desired shape to a large degree. Overall this confirms the favourable buildability this batch exhibits. Issues were, however, observed with printability and workability. As shown in figure 3a, constant extrusion was not achieved throughout the entire duration of printing which resulted in gaps in the object. Workability issues were also present during mixing and when loading the material into the cartridge.

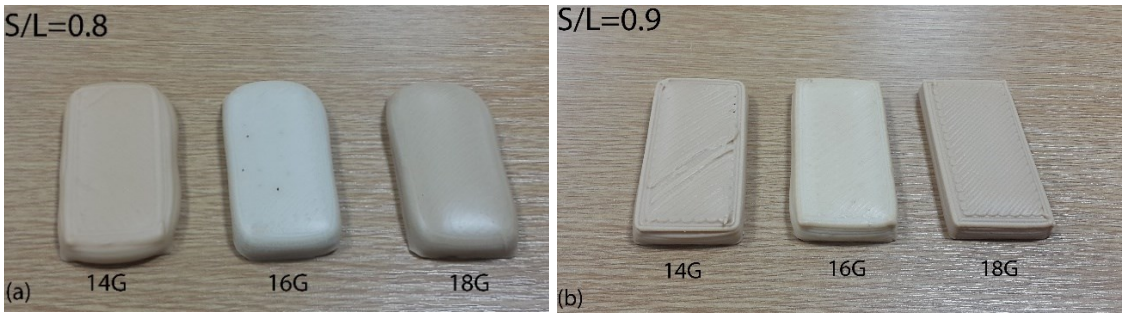

Figure 2. Printed samples a) wet batch b) dry batch

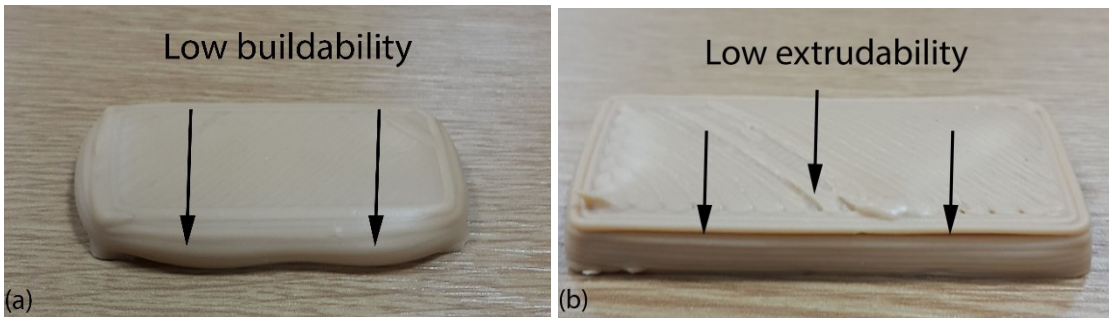

Figure 3. Printing issues a) low buildability for wet batch b) Low extrudability for dry batch

3.1.2 Nozzle size

As depicted in figure 2a nozzle sizes had little impact on the printed object in the wet batch. However, in the dry batch a smaller nozzle size slightly improved the final outcome in terms of detail as seen in figure 2b.

3.1.3 Optimal parameters

Upon completing the parameter selection stage, it was clear that each batch had its drawbacks. Buildability was the major issue with the wet batch while workability and extrudability were the main concerns of the dry batch. Open time was not considered an issue as the material was inserted immediately into the cartridge for extrusion following mixing. While the dry batch was seemingly the better option at first, its inconsistency in continuous printing, and its viscous nature were matters that could affect repeatability. As such, it was decided that the ideal mix should attain attributes of both batches to compensate for each of their drawbacks. Consequently, an intermediate ratio (S/L=0.85)

was selected. The nozzle size chosen was 18G to improve the printing resolution, as outlined in Section 3.1.2.

Figure 4 depicts a printed object with this optimised configuration. Extrudability issues were not observed and the geometry was replicated to a satisfactory extent. This mix did showcase slight buildability issues, but this could also be attributed to the fact the object was being extruded onto an uneven surface due to the presence of the electrodes.

Figure 4. Optimal mix impedance setup

3.2 EIS response

Figures 5a and 5b display the electrical response of the printed sample for a frequency range of 0.1 Hz-1 MHz for two days. As it could be seen, changes appeared in both the Bode plot and the Nyquist plot during this time period. This could be justified by the continuous maturation of the cementitious material[24].

Furthermore, figures 6a and 6b display the variation of the two graphs upon load application. The load was applied on the first day of testing. The impact of load cannot be detected in the Bode plot but rather in the Nyquist plot. A shift in resistance was detected for loaded against unloaded conditions. This implies strain detection could be carried out for 3D printed patches, even by interrogating at a single arc frequency.

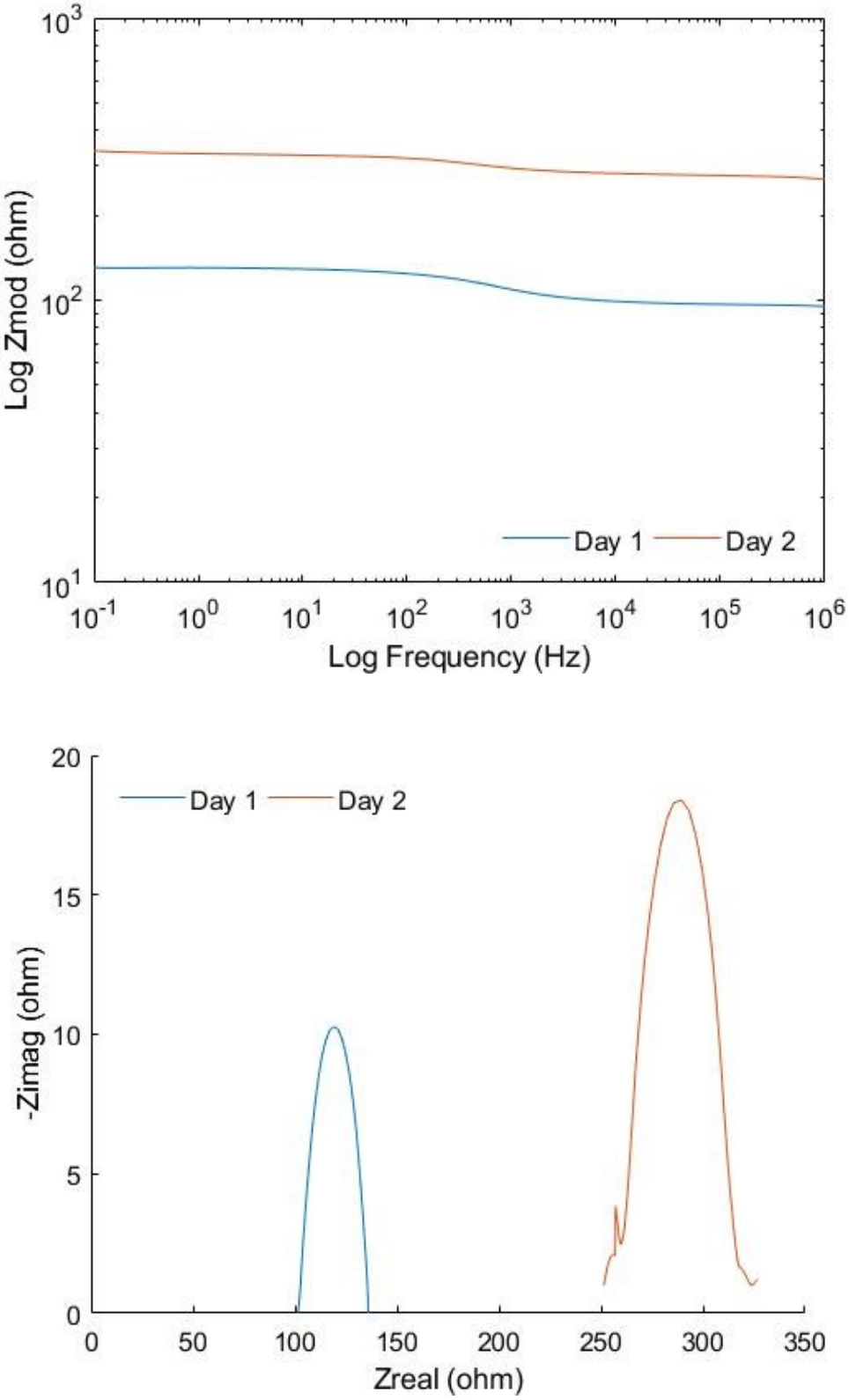

Figure 5. Impedance response of printed sample for two days a) Bode plot b) Nyquist plot

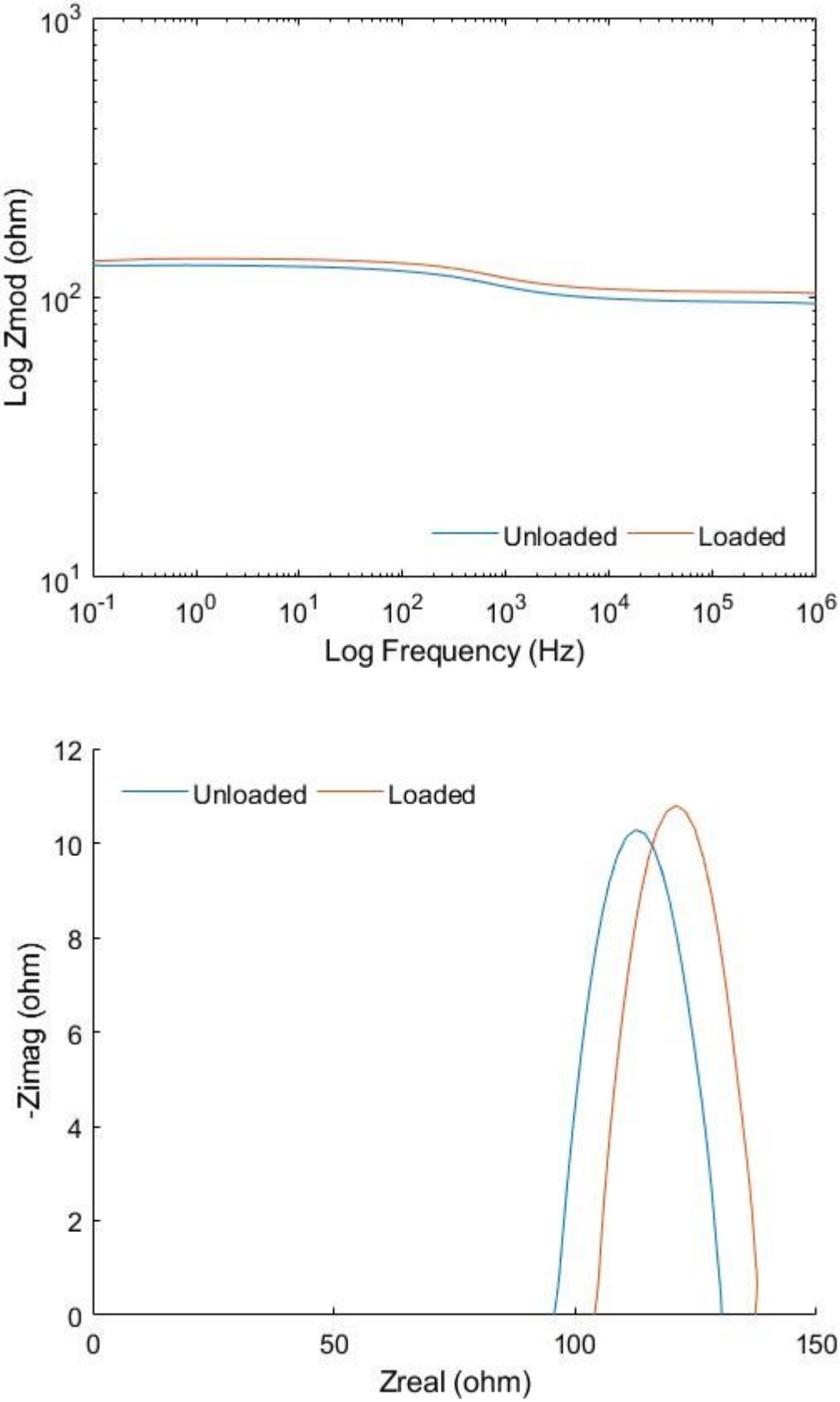

Figure 6. Impedance response of printed patch for load and unloaded conditions for day 1. a) Bode plot b) Nyquist plot

3.3 Future work

3.3.1 Cracks

In some printing attempts, cracks appeared in the sample as depicted in figure 7. These cracks were most likely caused by the presence of the electrodes[25]. It is worth noting that cracks can also appear in metakaolin-based geopolymers when not properly cured[26]. While meeting ideal curing condition can eliminate cracks, the actual behaviour of the material should also be taken into account[27]. Cracks can provide misleading measurements if the nature of these cracks is not clear (cracks due to strain or curing). Therefore, more research needs to be done to meet field application requirements.

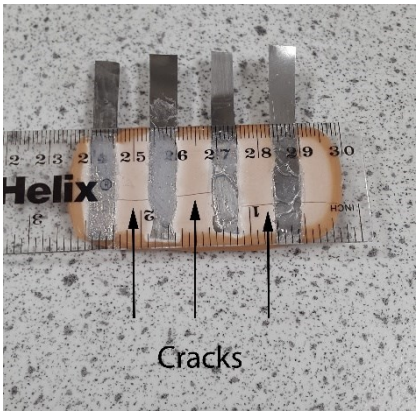

Figure 7. Cracked printed specimen

3.3.2 *Mix requirements*

More water makes for a more workable mix, but at the expense of strength and buildability. For this reason, a mix is required which is workable and extrudable without sacrificing buildability and strength. The process of determining the ideal mix is essentially a constant trial and error procedure[28].

3.3.3 3D printing

In the current experimental setup, a limited amount of material is allowed for extrusion. This essentially restricts the size of the printed object. Moreover, changing the cartridge and adding new material is not a practical option as residual material from the previous batch will still be present in the dispenser.

Finally factors such as 3D printing settings also need to be taken into consideration. Settings can influence aspects such as stability and strength[29,30]. However, it is yet unclear how these settings could affect impedance measurements.

4. Conclusion

In this research a geopolymer patch was extruded and tested for impedance. An optimal mix was reached that satisfied additive manufacturing requirements. The patch's electrical response changed between two days due to material maturing. In addition, load application was detected in impedance measurements.

Acknowledgments

This work was partly supported by the Royal Society, grant number RG160748.

References

1. McLellan BC, Williams RP, Lay J, Van Riessen A, Corder GD. Costs and carbon emissions for geopolymer pastes in comparison to ordinary portland cement. J Clean Prod [Internet]. 2011;19(9–10):1080–90. Available from: http://dx.doi.org/10.1016/j.jclepro.2011.02.010
2. Van Deventer JSJ, Provis JL, Duxson P. Technical and commercial progress in the adoption of geopolymer cement. Miner Eng [Internet]. 2012;29:89–104. Available from: http://dx.doi.org/10.1016/j.mineng.2011.09.009
3. Provis JL, Bernal SA. Geopolymers and Related Alkali-Activated Materials. Annu Rev Mater Res [Internet]. 2014;44(1):299–327. Available from: http://www.annualreviews.org/doi/10.1146/annurev-matsci-070813-113515
4. Davidovits J. Geopolymers: inorganic polymeric new materials. J Therm Anal. 1991;37(8):1633–56.
5. Provis JL. Geopolymers and other alkali activated materials: Why, how, and what? Mater Struct Constr. 2014;47(1–2):11–25.
6. Duxson P, Fernández-Jiménez A, Provis JL, Lukey GC, Palomo A, Van Deventer JSJ. Geopolymer technology: The current state of the art. J Mater Sci. 2007;42(9):2917–33.
7. Provis J. Activating solution chemistry for geopolymers. In: Geopolymers: Structure, processing, properties and industrial applications. Provis J, van Deventer J, editors. Cambridge: Woodhead; 2009. 50-71 p.
8. Rashad AM. Metakaolin as cementitious material: History, scours, production and composition-A comprehensive overview. Constr Build Mater [Internet]. 2013;41:303–18. Available from: http://dx.doi.org/10.1016/j.conbuildmat.2012.12.001
9. Provis JL, Duxson P, van Deventer JSJ. The role of particle technology in developing sustainable construction materials. Adv Powder Technol [Internet]. 2010;21(1):2–7. Available from: http://dx.doi.org/10.1016/j.apt.2009.10.006
10. Kong DLY, Sanjayan JG, Sagoe-Crentsil K. Factors affecting the performance of metakaolin geopolymers exposed to elevated temperatures. J Mater Sci [Internet]. 2008;43(3):824–31. Available from: http://link.springer.com/10.1007/s10853-007-2205-6
11. Huseien GF, Mirza J, Ismail M, Ghoshal SK, Abdulameer Hussein A. Geopolymer mortars as sustainable repair material: A comprehensive review. Renew Sustain Energy Rev [Internet]. 2017;80(April):54–74. Available from: http://dx.doi.org/10.1016/j.rser.2017.05.076
12. Romagnoli M, Leonelli C, Kamse E, Lassinantti Gualtieri M. Rheology of geopolymer by DOE approach. Constr Build Mater [Internet]. 2012;36:251–8. Available from: http://dx.doi.org/10.1016/j.conbuildmat.2012.04.122
13. Alonso MM, Gismera S, Blanco MT, Lanzón M, Puertas F. Alkali-activated mortars: Workability and rheological behaviour. Constr Build Mater [Internet]. 2017;145:576–87. Available from: http://dx.doi.org/10.1016/j.conbuildmat.2017.04.020

14. He J, Zhang G, Hou S, Cai CS. Geopolymer-Based Smart Adhesives for Infrastructure Health Monitoring: Concept and Feasibility. J Mater Civ Eng. 2011;23(February):100–9.
15. Saafi M, Tang L, Fung J, Rahman M, Sillars F, Liggat J, et al. Graphene/fly ash geopolymeric composites as self-sensing structural materials. Smart Mater Struct. 2014;23(6).
16. Perry M, Saafi M, Fusiek G, Niewczas P. Geopolymeric thermal conductivity sensors for surface-mounting onto concrete structures. 2016;(2014).
17. Cui XM, Zheng GJ, Han YC, Su F, Zhou J. A study on electrical conductivity of chemosynthetic Al2O3-2SiO2geoploymer materials. J Power Sources. 2008;184(2):652–6.
18. Hanjitsuwan S, Chindaprasirt P, Pimraksa K. Electrical conductivity and dielectric property of fly ash geopolymer pastes. Int J Miner Metall Mater. 2011;18(1):94–9.
19. Vaidya S, Allouche EN. Strain sensing of carbon fiber reinforced geopolymer concrete. Mater Struct [Internet]. 2011;44(8):1467–75. Available from: http://www.springerlink.com/index/10.1617/s11527-011-9711-3
20. Wu P, Wang J, Wang X. A critical review of the use of 3-D printing in the construction industry. Autom Constr [Internet]. 2016;68:21–31. Available from: http://dx.doi.org/10.1016/j.autcon.2016.04.005
21. Le TT, Austin SA, Lim S, Buswell RA, Gibb AGF, Thorpe T. Mix design and fresh properties for high-performance printing concrete. Mater Struct Constr. 2012;45(8):1221–32.
22. Lim S, Buswell RA, Le TT, Austin SA, Gibb AGF, Thorpe T. Developments in construction-scale additive manufacturing processes. Autom Constr. 2012;21(1):262–8.
23. Guo W, Wu G, Wang J, Wen Z, Yin S. Preparation and performance of geopolymers. J Wuhan Univ Technol Mater Sci Ed. 2008;23(3):326–30.
24. Gu P, Xie P, Beaudoin JJ, Brousseau R. A.C. impedance spectroscopy (I): A new equivalent circuit model for hydrated portland cement paste. Cem Concr Res. 1992;22(5):833–40.
25. Tang SW, Cai XH, He Z, Zhou W, Shao HY, Li ZJ, et al. The review of pore structure evaluation in cementitious materials by electrical methods. Constr Build Mater. 2016;117:273–84.
26. Perera DS, Uchida O, Vance ER, Finnie KS. Influence of curing schedule on the integrity of geopolymers. J Mater Sci. 2007;42(9):3099–106.
27. Bernal SA, Provis JL. Durability of alkali-activated materials: Progress and perspectives. J Am Ceram Soc. 2014;97(4):997–1008.
28. Panda B, Tan MJ. Experimental study on mix proportion and fresh properties of fly ash based geopolymer for 3D concrete printing. Ceram Int [Internet]. 2018;(March):0–1. Available from: http://linkinghub.elsevier.com/retrieve/pii/S0272884218305819
29. Panda B, Paul SC, Mohamed NAN, Tay YWD, Tan MJ. Measurement of tensile bond strength of 3D printed geopolymer mortar. Meas J Int Meas Confed [Internet]. 2018;113(April 2017):108–16. Available from: http://dx.doi.org/10.1016/j.measurement.2017.08.051
30. Bos F, Wolfs R, Ahmed Z, Salet T. Additive manufacturing of concrete in construction: potentials and challenges of 3D concrete printing. Virtual Phys

Prototyp. 2016;11(3):209–25.